molecular pharmaceutics

ARTICLE

pubs.acs.org/molecularpharmaceutics

Early Detection and Treatment of Wear Particle-Induced Inflammation and Bone Loss in a Mouse Calvarial Osteolysis Model Using HPMA Copolymer Conjugates

Ke Ren,[†] P. Edward Purdue,[‡] Lyndsey Burton,[‡] Ling-dong Quan,[†] Edward V. Fehringer,[§] Geoffrey M. Thiele,[∥,⊥,#] Steven R. Goldring,[‡] and Dong Wang*[,†]

[†]Department of Pharmaceutical Sciences, University of Nebraska Medical Center, Omaha, Nebraska 68198, United States

[‡]Hospital for Special Surgery, 535 East 70th Street, New York, New York 10021, United States

[§]Department of Orthopedic Surgery and Rehabilitation, University of Nebraska Medical Center, Omaha, Nebraska 68198, United States

[∥]Department of Internal Medicine, Division of Rheumatology, University of Nebraska Medical Center, Omaha, Nebraska 68198, United States

[⊥]Department of Pathology and Microbiology, University of Nebraska Medical Center, Omaha, Nebraska 68198, United States

[#]Omaha VA Medical Center, 4101 Woolworth Avenue, Omaha, Nebraska 68105, United States

Supporting Information

ABSTRACT: Wear particle-induced inflammation is considered to be the major cause of aseptic implant loosening and clinical failure after total joint replacement. Due to the frequent absence of symptoms, early detection and intervention prior to implant failure presents a significant challenge. To address this issue, a *N*-(2-hydroxypropyl)methacrylamide (HPMA) copolymer-based optical imaging contrast agent (P-IRDye) was developed and used for the detection of wear particle-induced inflammation employing a murine calvaria osteolysis model. The particle-induced osteolysis of calvaria was evaluated by H&E, tartrate-resistant acid phosphatase (TRAP) staining and μ-CT after necropsy. One-day post particle implantation, P-IRDye was administrated to the mice via tail vein injection. Live imaging of the animals 6 days after implantation revealed the preferential distribution and sustained retention of the macromolecular contrast agent at the site of particle implantation. Immunohistochemical staining and FACS analyses of the calvaria-associated soft tissue revealed extensive uptake of the HPMA copolymer by F4/80, Ly-6G (Gr1) and CD11c positive cells, which accounts for the retention of the macromolecular probes at the inflammatory sites. To test the potential of the system for therapeutic intervention, an acid-labile HPMA copolymer−dexamethasone conjugate (P-Dex) was prepared and shown to prevent the particle-induced inflammation and bone damage in the calvaria osteolysis model.

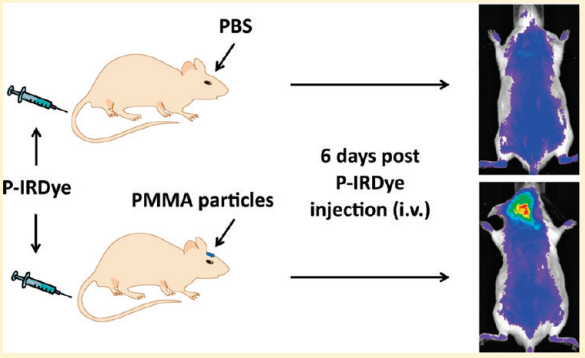

KEYWORDS: HPMA copolymer, aseptic orthopedic implant loosening, theranostics, orthopedic wear particle, inflammation targeting

1. INTRODUCTION

It is estimated that 1.5 million total joint arthroplasty procedures are performed annually worldwide to treat end-stage joint disease.[1] The overall 10-year success rate for total joint replacement is 90% with close to 10% of patients requiring revision surgery, which is associated with a poorer outcome and a shorter duration of implant survival.[2] Clinically, imaging modalities such as successive X-ray, CT and MRI have been used in the diagnosis of osteolysis and implant loosening.[3] These methods are very effective in detecting established bone deterioration and associated loss of implant fixation. However, due to the nature of these diagnostic tools, they only reveal anatomical alteration within the limit of the imaging resolution. When pain or clear radiographic evidence is reported, unfortunately, considerable bone loss has already occurred, which cannot be easily restored. Therefore, there is an urgent need for novel methodologies to report early biological events that precede the development of extensive osteolysis and the eventual loss of implant fixation.

Special Issue: Molecular Pharmaceutical Strategies for Improved Treatment of Musculoskeletal Diseases

Received: February 1, 2011
Accepted: March 25, 2011
Revised: March 16, 2011
Published: March 25, 2011

dx.doi.org/10.1021/mp2000555 | *Mol. Pharmaceutics* 2011, 8, 1043–1051

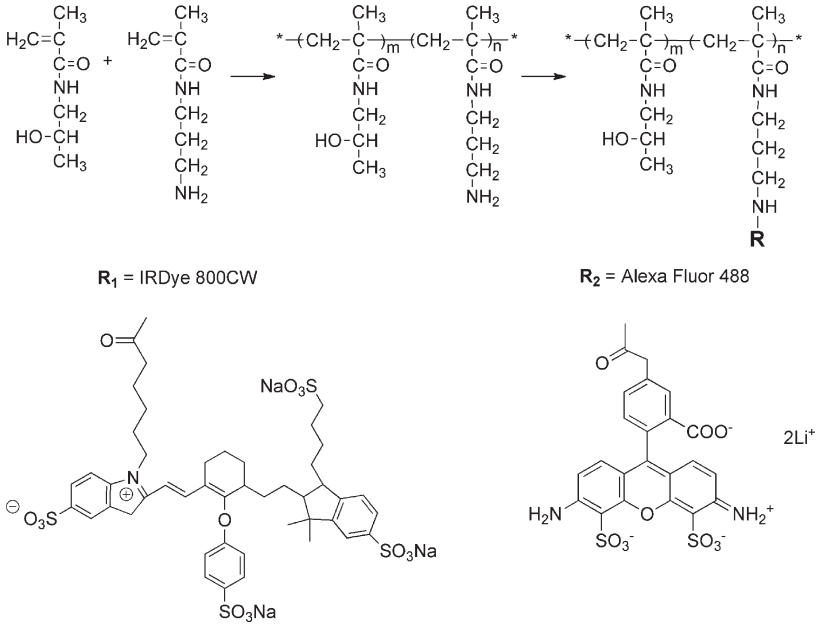

Figure 1. The syntheses of P-IRDye and P-Alexa.

Current understanding of the etiology of implant loosening suggests that inflammation caused by wear particles generated from the articulating surfaces of the prosthetic components is the major cause of aseptic implant loosening and clinical failure after total joint replacement.[4] Wear particles have been shown to activate macrophages and induce a granulomatous inflammatory reaction that results in osteoclast-mediated peri-implant osteolysis at the bone−implant interface, leading to the loss of the implant fixation. An imaging technology that could detect this inflammatory event would provide a unique opportunity for the early diagnosis of implant loosening. Subsequent therapeutic interventions at this stage would permit prolongation of the lifetime of the implant with improved patient outcomes.

Recently, data from our laboratories have demonstrated that *N*-(2-hydroxypropyl)methacrylamide (HPMA) copolymer−drug conjugates[5] could effectively target a site of inflammation after systemic administration and provide sustained amelioration in an inflammatory arthritis rat model. A detailed dissection of the mechanism suggests that the targeting and retention of the macromolecules at the inflammatory sites are due to their extravasation through leaky vasculature and subsequent inflammatory cell-mediated sequestration.[6,7] Based on these findings, we hypothesized that the HPMA copolymer could target sites of inflammation induced by wear particles, and when conjugated with an imaging agent, the HPMA copolymers could detect the local particle-induced inflammation as an early predictor of implant loosening. Additionally, we hypothesized that a potent anti-inflammatory agent could be conjugated to the copolymer, thereby providing a drug delivery system that concentrates the therapeutic agent at the site of inflammation, resulting in a sustained and more effective therapeutic effect with potentially reduced systemic adverse events.

2. MATERIALS AND METHODS

2.1. Synthesis of HPMA Copolymer Conjugates. *Synthesis of Poly(HPMA-co-APMA).* HPMA (1 g, 6.98 mmol),[8] *N*-(3-aminopropyl)methacrylamide hydrochloride (APMA, 12.5 mg, 0.07 mmol, Polysciences, Inc., Warrington, PA), azobisisobutyronitrile (AIBN, 6.74 mg, Sigma-Aldrich, Milwaukee, WI), *S*,*S*′-bis(α,α′-dimethyl-α″-acetic acid)-trithiocarbonate[9] (CTA, 6.26 mg, purity >97%) and *N*-methacryloylaminopropyl fluorescein thiourea[10] (MA-FITC, 4 mg) were dissolved in methanol (8 mL), placed in an ampule, and purged with N_2 for 5 min. The ampule was flame-sealed and maintained at 40 °C for 48 h in darkness. The product was purified by LH-20 column (GE HealthCare, Piscataway, NJ) to remove the unreacted low molecular weight compounds and then lyophilized. The final yield was 0.42 g. The amine content of the copolymer was determined as 2.7×10^{-5} mol/g using the ninhydrin assay.[11] The apparent weight average molecular weight (M_w = 3.71 × 10^4 kDa) and number average molecular weight (M_n = 2.65 × 10^4 kDa) of copolymers were determined based on a HPMA homopolymer calibration using an ÄKTA FPLC system (GE HealthCare, Piscataway, NJ) equipped with UV and RI detectors.

Synthesis of IRDye 800CW-Labeled HPMA Copolymer (Figure 1). Poly(HPMA-*co*-APMA) (16.5 mg, containing 0.00044 mmol of primary amine), IRDye 800CW NHS ester (0.5 mg, 0.00043 mmol, LI-COR Biosciences, Lincoln, NE) were dissolved in dimethylformamide (DMF, 300 μL) with *N*,*N*-diisopropylethylamine (DIPEA, 5 μL) added. The solution was stirred overnight in darkness at room temperature. The product was then purified on a LH-20 column and lyophilized. The final product yield was 15.02 mg. The IRDye 800CW content was determined as 1.1×10^{-5} mol/g using a Lambda 10 UV/vis spectrometer (PerkinElmer, Shelton, CT).

Synthesis of Alexa Fluor 488-Labeled HPMA Copolymer (Figure 1). Poly(HPMA-*co*-APMA) (30.0 mg, 0.0008 mmol), Alexa Fluor 488 NHS ester (0.517 mg, 0.0008 mmol, Invitrogen, Camarillo, CA) was dissolved in DMF (0.5 mL) with DIPEA (5 μL) added. The mixture was stirred overnight in darkness at room temperature. The product was purified on an LH-20 column and lyophilized. The final product yield was 28.62 mg. The Alexa Fluor 488 content was determined as 1.9×10^{-5} mol/g using a Lambda 10 UV/vis spectrometer.

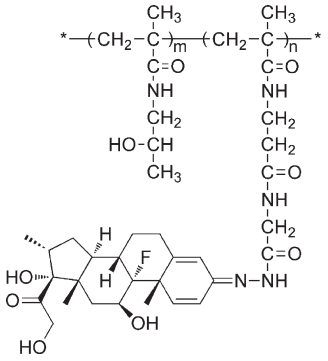

Figure 2. Chemical structure of P-Dex.

Synthesis of HPMA Copolymer—Dexamethasone Conjugate (P-Dex) (Figure 2). The synthesis of P-Dex and quantification of Dex loading in P-Dex were performed according to procedures described previously.[7]

2.2. Models. Two models were employed to induce inflammation and calvarial osteolysis:

Injection Model. To generate local inflammation and osteolysis for the imaging and histopathological and fluorescence-activated cell sorting (FACS) studies, poly(methyl methacrylate) (PMMA) particles (diameter at 1−10 μm, Bangs Laboratories, Fishers, IN) were soaked in 70% ethanol overnight, then washed and suspended in sterile phosphate-buffered saline (PBS) prior to implantation. A limulus assay was performed using a Pyrosate kit (Associates of Cape Cod, Inc., East Falmouth, MA) to confirm that the treated particles were endotoxin-free. Male Swiss Webster mice (6 weeks, Charles River Laboratories Inc., Wilmington, MA) were anesthetized with 70−80 mg/kg of ketamine and 5−7 mg/kg xylazine through intraperitoneal injection, and PBS (100 μL, for sham conrol) or PMMA (3 mg suspended in 100 μL of PBS) was deposited onto the calvarial surface through a 25G needle, which was inserted subcutaneously to the center of calvaria. This model was employed for these studies, since it, unlike the surgical model described below, produced minimal local trauma and tissue disruption that would confound interpretation of the results.

Surgical Insertion Model. Ultrahigh molecular weight polyethylene particles (UHMWPE) generated at Hospital for Special Surgery (HSS) were used to produce inflammation and osteolysis for the therapeutic intervention studies. Particles were soaked in 70% ethanol overnight and then washed and suspended in sterile PBS prior to use. The particles were allowed to dry in a desiccator and stored at 4 °C. Ultrasterile tubes were used during preparation and storage.

After anesthesia, the skin of Swiss Webster mice was shaved and sterilized. A 1.0 × 1.0 cm area of periosteum was exposed by making a 10 mm midline sagittal incision over the calvarium anterior to the line connecting both external ears using a scalpel. For osteolysis induction, the exposed calvarias were covered uniformly with 17 mg of UHMWPE particles suspended in 25 μL of PBS. The surgical incision was then closed with an EZ Clip Applier (Stoelting Co, IL). For sham control, sterile PBS (25 μL) without particles was used before closing the incision. The animals were returned to their cages after they were able to right themselves.

It needs to be noted that both PMMA and UHMWPE particles have been used in the mouse calvaria osteolysis model.[12,13] The particle size and morphology of the UHMWPE particles generated at HSS were similar to the wear particles found in human subjects undergoing revision surgery for aseptic loosening. As the UHMWPE particles tend to clump together in PBS and block their exit from the needle, PMMA particles were selected for the injection model. All of the animal experiments described above were performed according to a protocol approved by the University of Nebraska Medical Center Institutional Animal Care and Use Committee.

2.3. Near Infrared Optical Imaging of Mice with Mild Osteolysis. One-day post PMMA particle/PBS implantation, all mice were given IRDye 800CW-labeled HPMA copolymer (P-IRDye, 0.5 mg/mice) via tail vein injection. The mice were imaged prior to and daily after imaging agent injection using a XENOGEN IVIS 200 series imaging system (Hopkinton, MA) to evaluate the distribution of the P-IRDye continuously for the 6 days. The signal intensity was quantitatively analyzed by the resident software (Living Image, XENOGEN).

2.4. Histological Evaluation. For identification of osteoclasts, whole calvaria were fixed in 70% ethanol solution and then TRAP stained using a commercial staining kit (387A, Sigma-Aldrich, St. Louis, MO). Purple-stained cells are recognized as TRAP positive osteoclasts. For evaluation of bone resorption, the calvaria were fixed in 4% neutralized paraformaldehyde for 24 h and then decalcified in 10% EDTA (with 0.5% paraformaldehyde in PBS) at 4 °C for 2 weeks. The decalcification solution was changed every 2 days. The specimens were then paraffin embedded, sectioned (5 μm thickness) and H&E stained. The TRAP stained calvaria were examined with a precision stereo zoom microscope (PZMT III, World Precison Instrument, FL). The H&E stained sections were examined with an Olympus BX51 microscope (Olympus America Inc., Center Valley, PA).

2.5. Micro-CT Analyses. Mice were sacrificed in a carbon dioxide chamber seven days post particle/PBS implantation. The calvaria were removed by dissecting bone free from the underlying brain tissue and removing an elliptical plate of bone bound by the foramen magnum, auditory canals and orbits. They were stored in 70% ethanol and then scanned with a high-resolution micro-CT system (Skyscan 1172, Skyscan, Aartselaar, Belgium). The X-ray source was set at a voltage of 80 kV and a current of 100 μA with a fixed exposure time of 230 ms. Eight frames were averaged for each rotation with a rotation step of 0.9° following an angle of 180°. The resolution was 10 μm using medium camera pixel size (2000 × 1336) without filter. Three-dimensional reconstructions were performed by the system reconstruction software (NRecon, Skyscan). The analysis focused on the osseous properties in the center of the calvaria. A spherical region of interest (ROI) of 2 mm in diameter was defined as shown in Figure 8. For quantitative analysis of the particle-induced osteolysis, the resident software (CTAn, Skyscan) was used to obtain specific morphometric parameters within the ROI, such as bone volume (BV), tissue volume (TV) and bone volume density (BV/TV). 3D images of the calvaria were reconstructed using CT-vox software (Skyscan) to produce a visual representation of the results.

2.6. Immunohistochemical Analysis. To obtain sufficient tissue for immunohistochemical analysis and FACS analysis with the injection osteolysis model, 30 mg instead of 3 mg of PMMA particles was used. The surgical model was avoided to reduce the potential confounding effects of postsurgical inflammation related to the surgical trauma. Alexa Fluor 488-labeled HPMA copolymer (P-Alexa, 4.0 mg/mice) was given to mice by tail vein injection six days post particle implantation. At necropsy (24 h

post injection), the upper skull (including skin, underlying soft tissue and calvaria) was isolated as described above. The tissue was cut into two halves in the coronal plane centered over the area of particle deposition, and then immediately embedded in OCT compound and frozen with dry ice for frozen sectioning (7 μm thickness). The slides obtained were first incubated with 10% goat, rabbit or donkey serum (Sigma-Aldrich) for 30 min at room temperature. After addition of the primary antibodies {rabbit anti-mouse prolyl-4-hydroxylase (P4HB, Abcam, Cambridge, MA), rat anti-mouse F4/80 (Invitrogen, Camarillo, CA), rat anti-mouse Ly-6G (Gr-1, Gr1) (EBioscience, San Diego, CA) and Armenian hamster anti-mouse CD11c (BD Biosciences, Pharmingen, San Jose, CA), diluted in 10% corresponding blocking serum}, the sections were incubated at room temperature for 1 h in a humidified chamber. After washing with PBS, diluted secondary antibody {phycoerythrin (PE) labeled donkey anti-rabbit IgG (EBioscience), PE labeled goat anti-rat IgG (Invitrogen) or PE labeled rabbit anti-Armenian hamster IgG (EBioscience)} was added and incubated for another 30 min at room temperature in the dark. In control experiments, primary antibodies were replaced by corresponding isotype controls {purified rabbit IgG (Sigma-Aldrich), purified rat IgG (Sigma-Aldrich) and purified hamster IgG (Jackson ImmunoResearch, West Grove, PA)} and the samples were processed similarly as described above. The tissue sections were then evaluated with a Nikon Swept Field confocal microscope (Nikon Instruments Inc. Melville, NY). Representative micrographs were taken at a magnification of 400×.

2.7. Fluorescence-Activated Cell Scanning (FACS) Analysis. Similar to the immunohistochemistry study, P-Alexa (2.0 mg/mice) was given to mice by tail vein injection at six days post particle implantation. At necropsy (24 h post injection), soft tissues between skin and calvaria were isolated and minced aseptically. The tissues were further digested with type I collagenase (1 mg/mL, Sigma-Aldrich) at 37 °C for 2 h. After passing through a 70 μm cell strainer, a single cell suspension (1×10^6 cells/mL) was obtained. ACK Lysing Buffer (Quality Biological, Gaithersburg, MD) was then used to remove the red blood cells. For FACS evaluation of CD11c, F4/80 and Ly-6G (Gr-1, Gr1) positive cells, the samples were incubated with antibodies {allophycocyanin (APC)-labeled hamster anti-mouse CD11c (BD Biosciences, Pharmingen), PE-labeled rat anti-mouse F4/80 (AbD Serotec, Raleigh, NC), PE-labeled rat anti-mouse Ly-6G (Gr-1, Gr1) (EBioscience)} for 30 min on ice. For FACS evaluation of P4HB positive cells, the samples were first incubated with rabbit anti-mouse P4HB for 30 min on ice and then incubated with PE-labeled donkey anti-rabbit IgG for another 30 min on ice. Isotype-matched APC-labeled hamster IgG1 (BD Biosciences, Pharmingen), PE-labeled rat IgG2b (BD Biosciences, Pharmingen) and purified rabbit IgG were used as negative controls. After the final wash, the cells were analyzed with Becton Dickinson FACSCalibur flow cytometer (BD Biosciences, Pharmingen).

2.8. In Vivo Treatment Study. Twenty-five male Swiss Webster mice were randomly assigned into five groups. One group was designated as sham control without particle implantation. One-day post UHMWPE particle implantation, the animals in groups 2−5 were given the following treatments: group 2, free Dex (total dose = 20 mg/kg, four iv injections on four successive days); group 3, P-Dex (equivalent Dex dose = 20 mg/kg, single iv injection); group 4, PBS (single iv injection); group 5, HPMA homopolymer without Dex (PHPMA, single iv injection; amount of polymer used is equivalent to P-Dex). At 6 days post-treatment, the mice were euthanized and the upper skulls of the animals were isolated. Calvaria were then fixed with 70% ethanol and subjected to micro-CT analysis and whole calvaria TRAP staining as described previously.

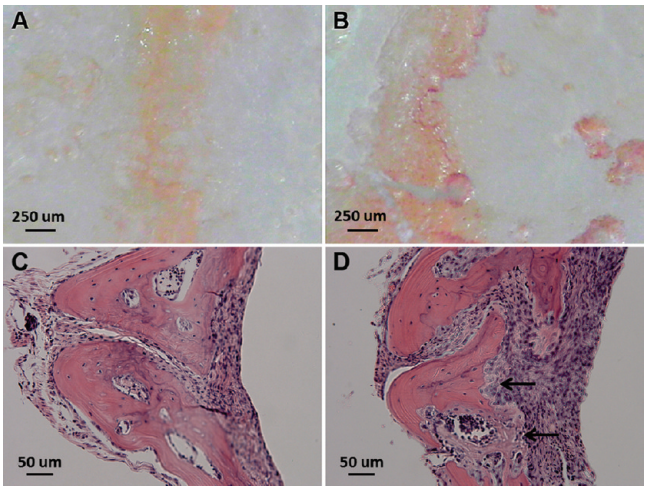

Figure 3. Representative images of undecalcified calvaria after TRAP-staining (A and B) and H&E stained decalcified calvaria tissue sections (C and D). Panels A and C are from mouse calvaria injected with PBS, while B and D are from animals implanted with PMMA particles. TRAP-staining of the undecalcified calvarial tissue shows the presence of abundant TRAP-positive cells from the PMMA particle implanted animal (panel B). The arrows in panel D indicate the region of focal bone resorption.

2.9. Statistical Methods. Comparisons between two groups for imaging study were performed using Student's t test: two-sample two-tails assuming equal variances. Statistical analysis among groups for the treatment study was performed by one-way ANOVA, followed by a post hoc test (Student−Newman−Keuls) for multiple comparisons. Data were expressed as means ± standard deviation. A p value of less than 0.05 is considered as statistically significant.

3. RESULTS

3.1. Assessment of Bone Resorption in the Mouse Calvaria Osteolysis Injection Model. As shown in Figure 3B, multiple TRAP-positive cells were present on the bone surfaces at the sites of PMMA particle implantation, consistent with active osteoclastic bone resorption. H&E staining of decalcified calvaria at the PMMA deposition sites revealed the presence of an intense inflammatory cell infiltrate and osteolysis (Figure 3D). Mice with calvarial injection of PBS exhibited no evidence of TRAP staining or inflammatory cell infiltration. Although there was histological evidence of osteolysis in this injection model, micro-CT analysis showed no significant difference ($p > 0.05$) in terms of BV/TV (%) between PBS and PMMA particle implantation groups.

3.2. Near-Infrared Optical Imaging of Mouse Calvaria Osteolysis Injection Model. A strong near-infrared (NIR) signal from the P-IRDye was associated with the PMMA particle deposition site 2 days post particle implantation (Figure 4). Daily imaging demonstrated the persistence of the P-IRDye signal for over 7 days. Quantitative analysis of the NIR signal intensity confirmed that at 7 days post P-IRDye administration ~60% of the signal remained, consistent with retention of P-IRDye at the PMMA particle

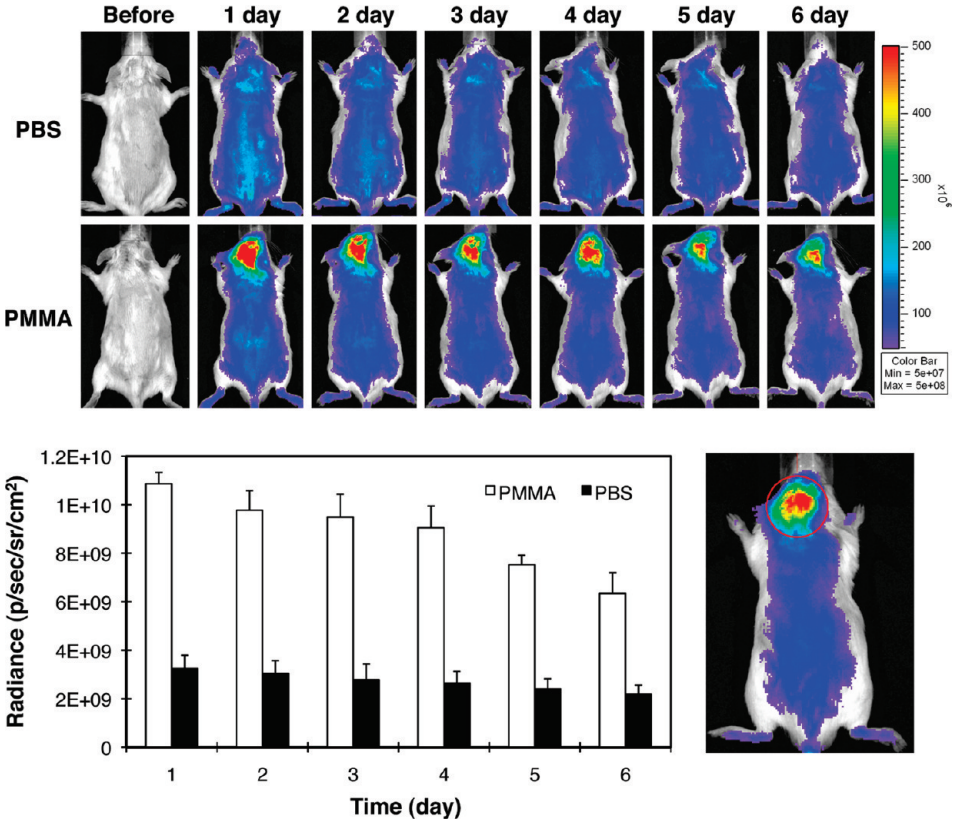

Figure 4. Live optical imaging after PBS or PMMA implantation. P-IRDye was given via tail vein injection the following day after PBS or PMMA implantation. The mice were imaged prior and each day after the administration of the optical imaging agent for the following 6 days ($n = 3$). (A) The upper panel shows the images from the mice with calvarial injection of PBS. The lower panel shows the images from the mice with calvarial PMMA-particle implantation. Compared to the PBS group, PMMA particle implanted animals demonstrated more intense and longer lasting NIR signals in the calvarial region where the PMMA particles were implanted. (B) The NIR signal intensity was measured from a consistent region of interest (red circle) in the calvaria site for all the mice. The signal intensity differences in the two groups were statistically significant ($p < 0.05$).

implantation site. The distribution and retention of the P-IRDye were significantly lower in the mice with calvarial PBS injection when compared to those implanted with PMMA particles ($p < 0.05$).

3.3. Immunohistochemical Analysis of Implantation Site Frozen Sections after PMMA Injection. As shown in Figure 5, immunohistochemical staining with anti-F4/80, anti-CD11c, anti-Ly-6G (Gr-1, Gr1) or anti-P4HB antibodies of the frozen sections from the mouse calvaria tissue from PMMA implanted animals revealed that many P-Alexa-positive cells stained positively for Ly-6G(Gr-1, Gr1) (monocyte marker) or F4/80 (macrophage marker). CD11c (dendritic cell marker) positive cells were either weakly positive or negative for P-Alexa staining, whereas P4HB (fibroblast marker) positive cells were negative.

3.4. FACS Analysis of Cells Isolated from PMMA Implantation Sites. FACS analysis revealed that more than 80% of the cells isolated from the inflammatory sites were Ly-6G (Gr-1, Gr1) positive and, of these cells, ~18% were P-Alexa positive. As shown in Figure 6, 25.1% of the P-Alexa positive cells were F4/80 positive; 35.15% of the P-Alexa positive cells were Ly-6G (Gr-1, Gr1) positive and 9.73% of the P-Alexa positive cells were CD11c positive. All data presented were isotype-control corrected. The study was repeated with P-Alexa administration on day 1 post PMMA particle implantation and tissue isolation and processing on day 7 post particle implantation. Though the overall P-Alexa positive cell numbers were reduced, they were still identified as F4/80, Ly-6G or CD11c positive with a similar ratio (data not shown).

3.5. Effects of P-Dex Treatment in UHMWPE Implantation Model. The therapeutic effect of P-Dex on osteolysis was evaluated by micro-CT and whole calvaria TRAP staining. As shown in Figure 7, multiple TRAP-positive cells were present on the bone surfaces in UHMWPE + PBS and UHMWPE + PHPMA groups, consistent with active osteoclastic bone resorption. The calvarial bones from UHMWPE + PBS treated mice (Figure 8C) exhibited evidence of significant bone loss compared to sham operated mice (Figure 8B) with lower mean BV/TV (%) values (2.3017 ± 0.1326 for UHMWPE/PBS treated mice compared to 2.6905 ± 0.1350 for sham mice). PHPMA alone did not prevent the UHMWPE-induced osteolysis (Figure 8D) or reduction in BV/TV (2.3017 ± 0.1326 for UHMWPE/PBS treated mice compared to 2.3254 ± 0.0766 for UHMWPE/HPMA treated mice). In contrast, UHMWPE + Dex (Figure 8E) and UHMWPE + P-Dex (Figure 8F) groups showed no evidence of osteolysis and maintained higher mean BV/TV (%) values of 2.6564 ± 0.1689 and 2.6161 ± 0.1064, respectively (Figure 9). The statistical analyses indicated that the average BV/TV (%) values of sham control, Dex treated and P-Dex treated groups were significantly higher ($p < 0.05$) than those of the PBS and PHPMA treatment groups. There were no significant differences among sham control, Dex treated and P-Dex treated groups ($p > 0.05$). The difference between PHPMA and PBS groups was not significant ($p > 0.05$).

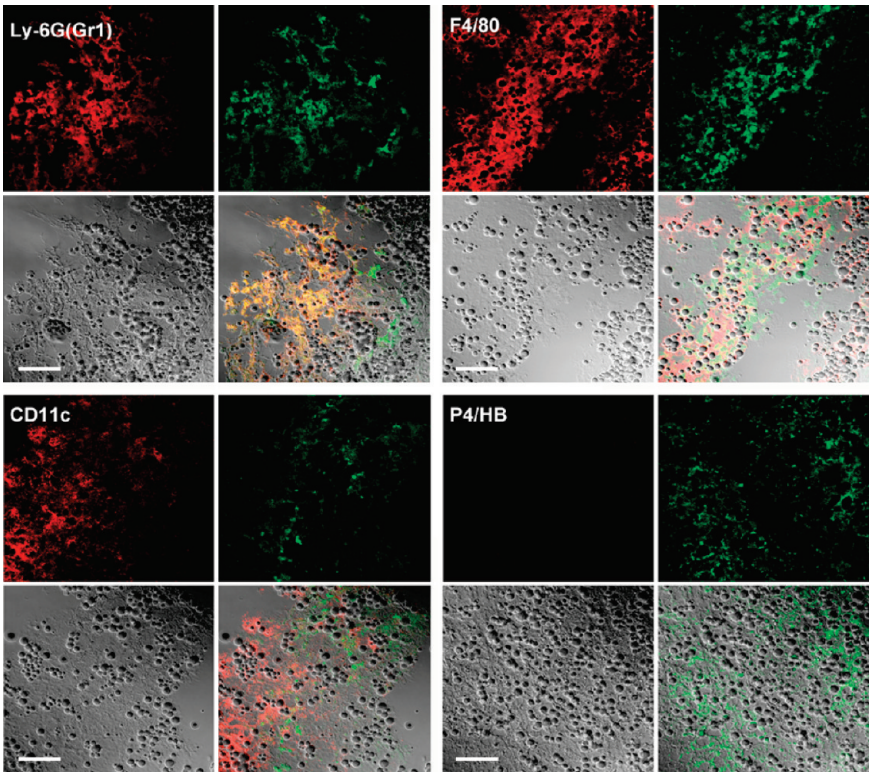

Figure 5. Representative confocal images of anti-Ly-6G (Gr-1, Gr1), anti-F4/80, anti-CD11c and anti-P4HB antibody stained frozen sections of calvaria and adjacent soft tissue from PMMA particle implanted mice (treated with P-Alexa). Each panel was composed of four subimages: antibody red staining, P-Alexa green fluorescence, DIC image and the colocalization of the three. The colocalization of red and green color in both panels yields a yellow color, which confirms the internalization of the HPMA copolymer conjugate by Ly-6G (Gr-1, Gr1), F4/80 or CD11c positive cells at the sites of inflammation. The spherical structures are PMMA particles. Bar = 50 μm.

4. DISCUSSION

The present study was undertaken to develop a diagnostic tool for the early detection of prosthetic implant wear particle-induced peri-implant inflammation. In addition, we hypothesized that this system could be adapted for delivery of therapeutic agents to attenuate the inflammatory response to wear particles and avert the development of peri-implant osteolysis and implant loosening. By conjugating an imaging probe or therapeutic agent to the copolymer, we showed that this system could be utilized as a theranostic platform[14,15] for both imaging and drug delivery functions.

In order to explore the potential of using HPMA copolymer-based imaging contrast agents for early identification of inflammation associated with orthopedic wear particles, we modified a standard mouse calvaria osteolysis surgery model, which has been widely used for the study of aseptic implant loosening.[16,17] In the surgery model, a midline sagittal incision is made to allow calvaria exposure, followed by particle deposition and incision closure. Two factors contribute to the inflammation at the implantation site, the natural repair of the surgical trauma and the cellular and tissue reaction to the implanted particles. To minimize the effects of the surgical trauma on local inflammation we opted to modify the open surgery procedure by using a minimally invasive injection method to introduce small amounts of PMMA particles (3 mg) onto the mouse calvaria. This model had the advantage of inducing minimal surgical trauma and was therefore optimal for the diagnostic imaging studies. Micro-CT analysis suggests that the bone damage produced in this model is limited. Importantly, however, particle-induced calvarial osteolysis was present with this minimally invasive procedure, as confirmed by H&E and TRAP-staining. These characteristics may resemble the early stage of peri-implant inflammation and osteolysis development.[18] As discussed below, we employed the surgical incision model for the therapeutic intervention studies since it produced more significant osteolysis.

The *in vivo* optical imaging studies with the modified mouse calvaria osteolysis model revealed that P-IRDye was mainly localized to the PMMA particle implantation sites 7 days post particle implantation. Contrary to the observation with P-IRDye, dose equivalent free NIR dye did not show any preferential tissue uptake (data not shown). H&E stained tissue sections from the particle implantation sites revealed infiltration of abundant inflammatory cells. Daily imaging of the animals revealed that the P-IRDye signal at the particle implantation site was sustained during the entire course of the study, with a gradual decline to 60% of the original signal intensity by day 6 post P-IRDye administration. The sustained contrast signal level indicates the potential clinical utility of this diagnostic system since it provides an extended imaging window for detection. While this polymer-based imaging approach has great potential for the early diagnosis of implant associated inflammation, the selection of the near-infrared imaging probe needs to be adapted with alternative contrast agents for clinical application in human subjects due to the relatively poor tissue penetration capability of near-infrared signals, especially through mineralized tissues.[19,20] For example, gamma or positron emitters (e.g., ^{123}I, ^{111}In, ^{99m}Tc, ^{18}F, ^{64}Cu,

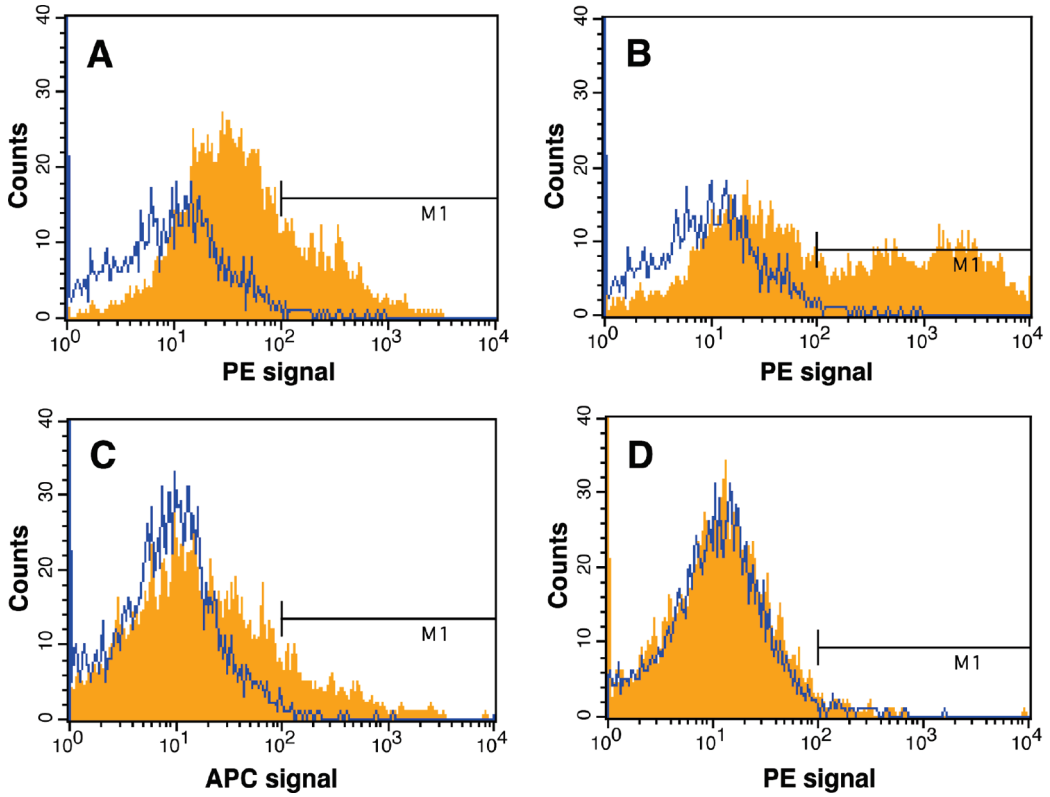

Figure 6. Representative data from fluorescence-activated cell scanning (FACS) analysis of cells isolated from sites of PMMA particle-induced inflammation 24 h after systemic administration of P-Alexa. The histogram plots show the intensity of staining with the specific antibodies designated on the *x*-axis (orange fills) with isotype control antibodies (blue lines) on the same plots. The percentages represent the percent of antibody positive cells among P-Alexa positive cells. (A) 25.12% P-Alexa positive cells were F4/80 positive; (B) 35.15% P-Alexa positive cells were Ly-6G positive; (C) 9.73% P-Alexa positive cells were CD11c positive; (D) < 1% P-Alexa positive cells were P4HB positive. Abundant spherical structures present in the tissue sections are PMMA particles.

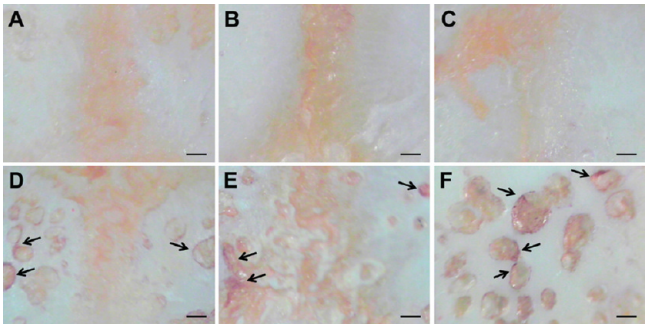

Figure 7. Representative images of TRAP-stained undecalcified calvaria from different treatment groups. (A) Sham control group; (B) UHMWPE + Dex group; (C) UHMWPE + P-Dex group; (D) UHMWPE + PHPMA group; (E) UHMWPE + PBS group. TRAP-positive areas (arrows) are abundant on calvaria surfaces from the PHPMA and PBS groups (midline region, magnifications are at 45×). Panel F focuses on a particular TRAP positive region of a calvarium from the PHPMA group. Bone resorption pits were visible surrounded by TRAP positive cells. Bar = 250 μm.

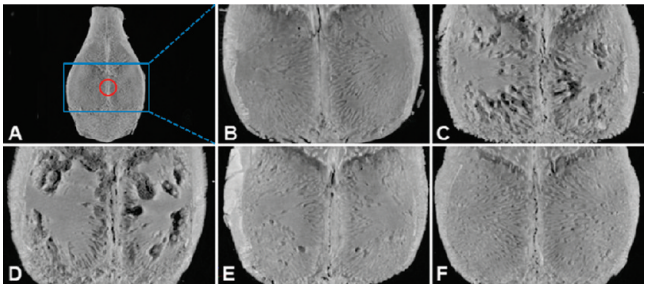

Figure 8. Representative micro-CT reconstructed images of the mouse calvaria after different treatments. The whole calvarium micro-CT image from a healthy (sham operated) mouse is shown in panel A. The red circle represents the spherical region of interest (ROI) of 2 mm in diameter in the center of calvarium used for quantitative analysis of BV/TV (%). Panels B to F show enlarged images of the selected blue square regions represented in panel A. (B) Sham control group (no particle); (C) UHMWPE + PBS group; (D) UHMWPE + PHPMA group; (E) UHMWPE + Dex group; (F) UHMWPE + P-Dex group. There was significant bone resorption in PBS and PHPMA treatment groups, while the UHMWPE-induced bone resorption was greatly attenuated in Dex and P-Dex treatment groups.

etc.) could be utilized in future studies in large animal or human clinical applications. Due to the high energy levels of these radioisotopes, their signals can be readily detected by clinical imaging modalities such as SPECT/CT and PET/CT.

Similar to the enhanced permeability and retention (EPR) effect observed with solid tumors,[21] increased vascular permeability to macromolecules has been well-documented with inflammatory tissues.[22] Different from solid tumors, however, the clearance of macromolecules from the interstitial space of inflammatory tissues proceeds rapidly and steadily via the

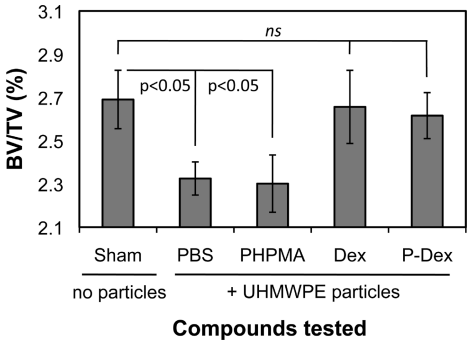

Figure 9. Quantitative analysis results of BV/TV (%) from micro-CT evaluation. Implantation of UHMWPE particles in vehicle (PBS) resulted in statistically significant reduction in BV/TV (%) values compared to sham control (no particles) ($p < 0.05$). Polymer alone (PHPMA) did not alter the UHMWPE-induced reduction in BV/TV. However, both Dex and P-Dex treatment groups significantly ($p < 0.05$) reversed the UHMWPE-induced reduction in BV/TV to levels comparable to sham mice; ns = not significant.

lymphatic system, after extravasation from blood vessels.[23] Our finding of the P-IRDye's sustained signal at the inflammatory sites in this study is of great interest since it suggests the presence of a previously unrecognized mechanism of macromolecule retention at sites of particle-induced inflammation. To explore this novel mechanism, mouse calvaria tissues associated with PMMA particles were isolated and processed for histological and FACS analyses. P-Alexa was used as a surrogate for P-IRDye as the near-infrared signal could not be detected by our confocal microscope and flow cytometer. To ensure similar physical—chemical properties of the two conjugates, the same amine-containing HPMA copolymer precursor used in the synthesis of P-IRDye was also used in the synthesis of P-Alexa. Immunohistological evaluation revealed that P-Alexa was internalized by cells at the inflammatory sites. Using a panel of antibodies, the cells were identified as macrophages ($F4/80^+$), dendritic cells ($CD11c^+$) or inflammatory monocytes ($Gr1^+$). Although Gr1 is also expressed on neutrophils, H&E staining (e.g., Figure 3D) confirmed that cells expressing phenotypic features of neutrophils were rarely detected. FACS analysis using specific neutrophil marker (rat anti-mouse neutrophils marker 7/4, AbD Serotec, Raleigh, NC) showed less than 5% percent of the P-Alexa positive cells were 7/4 positive (data not shown). Therefore, the GR1 and P-Alexa-positive cells were predominantly inflammatory monocytes. Analysis of the H&E tissue sections demonstrated that there were also cells with phenotypic features of fibroblasts, though P4HB positive cells were not detected in the immunohistological and FACS analyses, which may be attributed to the antigen denaturation during the tissue/cell processing. These findings suggest that the retention of the polymeric imaging probes is related to the cellular uptake of the copolymer by activated inflammatory cells after extravasation at the inflammatory site. Several questions remain concerning the process of cellular uptake and retention. For example, it is not clear if the polymer is retained in the endosomal/lysosomal compartment of the same cell or if the polymer is internalized and released by a cluster of activated inflammatory cells as a dynamic process.

Additional studies were undertaken to understand this novel inflammation targeting mechanism and to investigate if it could be exploited for delivery of a therapeutic moiety to impede the wear particle-induced inflammation and associated osteolysis. Dexamethasone was selected as the prototype anti-inflammation drug to be conjugated to the HPMA copolymer due to its potent anti-inflammatory efficacy. The micro-CT results demonstrated that administration of a single P-Dex injection one day after particle implantation attenuated osteolysis. No significant difference in BV/TV was found among sham control, UHMWPE + Dex and UHMWPE + P-Dex groups. The similar osteoprotective effect of P-Dex and Dex may be explained by the relatively high drug dose used in this study. Therefore, dose optimization needs to be performed in the future to further differentiate the therapeutic efficacy of P-Dex and Dex as we have observed in previous arthritis studies.[5,7,24] In addition, as the P-Dex treatment is primarily localized to the sites of the particle-induced inflammation, it is yet to be tested if P-Dex treatment could circumvent the systemic toxicity associated with free Dex treatment. *In vitro* cell culture studies showed that P-Dex was internalized by PMMA particle-activated human monocytes via endocytosis and that it was retained in a lysosomal compartment. This treatment was accompanied by the suppression of particle-induced expression of inflammatory cytokines such as IL-1α and IL-1β, which likely contribute to the attenuation of the local inflammatory response (data not shown). Suppression of expression of IL-1 and related inflammatory cytokines with osteoclast-inducing activity by the P-Dex provides a likely mechanism by which the P-Dex copolymer inhibited particle-induced osteolysis. This agrees with our previous findings[24] in which P-Dex treatment and cellular uptake by LPS-activated human monocytes and TNF-α-activated human fibroblast significantly reduced the capacity of these cells to produce inflammatory cytokines.

5. CONCLUSION

Using a modified murine calvarial osteolysis model, we show that imaging agents based on water-soluble macromolecules, such as HPMA copolymers, can be used to identify sites of inflammation associated with the early stage of particle-induced inflammation and subsequent osteolysis. Adaptation of this system for the use of high-energy radioisotopes instead of optical imaging probes will permit development of imaging tools for human application. Macromolecules were shown to extravasate at particle-induced inflammatory sites through the leaky vasculature and retained through inflammatory cell-mediated sequestration. Micro-CT analysis and whole calvaria TRAP staining demonstrated that systemic administration of HPMA copolymer—dexamethasone (a prototypical anti-inflammatory drug) conjugate (P-Dex) to the mouse calvarial osteolysis model was osteoprotective. Additional experiments are ongoing to investigate if the prodrug could reduce the systemic toxicity of Dex and if other anti-inflammatory agents that intervene with more specific molecular targets associated with inflammatory pathways (e.g., NF-κB) can be successfully targeted with this delivery platform.

■ ASSOCIATED CONTENT

Supporting Information. μ-CT reconstruction movies of representative calvaria from Sham control group (no particle), UHMWPE + PBS group, UHMWPE + PHPMA group, UHMWPE + Dex group and UHMWPE + P-Dex group. This material is available free of charge via the Internet at http://pubs.acs.org.

AUTHOR INFORMATION

Corresponding Author

*Department of Pharmaceutical Sciences, University of Nebraska Medical Center, 986025 Nebraska Medical Center, COP 3026, Omaha, NE 68198-6025, USA. Tel: +1 402-559-1995. Fax: +1 402-559-9543. E-mail: dwang@unmc.edu.

ACKNOWLEDGMENT

This study was supported in part by National Institutes of Health/National Institute of Arthritis, Musculoskeletal and Skin Diseases with Grant Number R01 AR053325 to D.W. and ACR-REF: Within Our Reach Grant to S.R.G.

REFERENCES

(1) Teeny, S. M.; York, S. C.; Mesko, J. W.; Rea, R. E. Long-term follow-up care recommendations after total hip and knee arthroplasty: results of the American Association of Hip and Knee Surgeons' member survey. *J. Arthroplasty* **2003**, *18* (8), 954–962.

(2) Amstutz, H. C.; Campbell, P.; Kossovsky, N. Mechanism and clinical significance of wear debris-induced osteolysis. *Clin. Orthop.* **1992**, 3 (276), 7–18.

(3) Leopold, S. S.; Rosenberg, A. G.; Bhatt, R. D.; Sheinkop, M. B.; Quigley, L. R.; Galante, J. O. Cementless acetabular revision. Evaluation at an average of 10.5 years. *Clin. Orthop. Relat. Res.* **1999**, *12* (369), 179–186.

(4) Holt, G.; Murnaghan, C.; Reilly, J.; Meek, R. M. The biology of aseptic osteolysis. *Clin. Orthop. Relat. Res.* **2007**, *7* (460), 240–252.

(5) Wang, D.; Miller, S. C.; Liu, X. M.; Anderson, B.; Wang, X. S.; Goldring, S. R. Novel dexamethasone-HPMA copolymer conjugate and its potential application in treatment of rheumatoid arthritis. *Arthritis Res. Ther.* **2007**, *9* (1), R2.

(6) Duncan, R. The dawning era of polymer therapeutics. *Nat. Rev. Drug Discovery* **2003**, *2* (5), 347–360.

(7) Liu, X. M.; Quan, L. D.; Tian, J.; Alnouti, Y.; Fu, K.; Thiele, G. M.; Wang, D. Synthesis and evaluation of a well-defined HPMA copolymer-dexamethasone conjugate for effective treatment of rheumatoid arthritis. *Pharm. Res.* **2008**, *25* (12), 2910–2919.

(8) Kopeček., J.; Bazilová, H. Poly[N-(2-hydroxypropyl)methacrylamide] — I. Radical polymerization and copolymerization. *Eur. Polym. J.* **1973**, *9* (1), 7–14.

(9) Lai, J. T.; Filla, D.; Shea, R. Functional polymers from novel carboxyl-terminated trithiocarbonates as highly efficient RAFT agents. *Macromolecules* **2002**, *35* (18), 6754–6756.

(10) Omelyanenko, V.; Kopečková, P.; Gentry, C.; Kopeček, J. Targetable HPMA copolymer-adriamycin conjugates. Recognition, internalization, and subcellular fate. *J. Controlled Release* **1998**, *53* (1−3), 25–37.

(11) Moore, S.; Stein, W. H. A modified ninhydrin reagent for the photometric determination of amino acids and related compounds. *J. Biol. Chem.* **1954**, *211* (2), 907–913.

(12) Landgraeber, S.; Jaeckel, S.; Löer, F.; Wedemeyer, C.; Hilken, G.; Canbay, A.; Totsch, M.; von Knoch, M. Pan-caspase inhibition suppresses polyethylene particle-induced osteolysis. *Apoptosis* **2009**, *14* (2), 173–181.

(13) Zhang, C.; Tang, T. T.; Ren, W. P.; Zhang, X. L.; Dai, K. R. Inhibiting wear particles-induced osteolysis with doxycycline. *Acta Pharmacol. Sin.* **2007**, *28* (10), 1603–1610.

(14) Sun, D. Nanotheranostics: Integration of Imaging and Targeted Drug Delivery. *Mol. Pharmaceutics* **2010**, *7* (6), 1879.

(15) Lammers, T.; Kiessling, F.; Hennink, W. E.; Storm, G. Nanotheranostics and Image-Guided Drug Delivery: Current Concepts and Future Directions. *Mol. Pharmaceutics* **2010**, *7* (6), 1899–1912.

(16) Kaar, S. G.; Ragab, A. A.; Kaye, S. J.; Kilic, B. A.; Jinno, T.; Goldberg, V. M.; Bi, Y.; Stewart, M. C.; Carter, J. R.; Greenfield, E. M. Rapid repair of titanium particle-induced osteolysis is dramatically reduced in aged mice. *J. Orthop. Res.* **2001**, *19* (2), 171–178.

(17) Von Knoch, F.; Wedemeyer, C.; Heckelei, A.; Saxler, G.; Hilken, G.; Brankamp, J.; Sterner, T.; Landgraeber, S.; Henschke, F.; Löer, F.; von Knoch, M. Promotion of bone formation by simvastatin in polyethylene particle-induced osteolysis. *Biomaterials* **2005**, *26* (29), 5783–5789.

(18) Katzer, A.; Lœhr, J. F. Early loosening of hip replacements: causes, course and diagnosis. *J. Orthop. Traumatol.* **2003**, *4* (3), 105–116.

(19) Kolari, P. J.; Airaksinen, O. Poor penetration of infra-red and helium neon low power laser light into the dermal tissue. *Acupunct. Electrother. Res.* **1993**, *18* (1), 17–21.

(20) Mancini, D. M.; Bolinger, L.; Li, H.; Kendrick, K.; Chance, B.; Wilson, J. R. Validation of near-infrared spectroscopy in humans. *J. Appl. Physiol.* **1994**, *77* (6), 2740–2747.

(21) Matsumura, Y.; Maeda, H. A new concept for macromolecular therapeutics in cancer chemotherapy: mechanism of tumoritropic accumulation of proteins and the antitumor agent smancs. *Cancer. Res.* **1986**, *46* (12), 6387–6392.

(22) Henson, P. M. Dampening inflammation. *Nat. Immunol.* **2005**, *6*, 1179–1181.

(23) Maeda, H. Tumor-selective delivery of macromolecular drugs via the EPR effect: background and future prospects. *Bioconjugate Chem.* **2010**, *21* (5), 797–802.

(24) Quan, L. D.; Purdue, P. E.; Liu, X. M.; Boska, M. D.; Lele, S. M.; Thiele, G. M.; Mikuls, T. R.; Dou, H.; Goldring, S. R.; Wang, D. Development of a macromolecular prodrug for the treatment of inflammatory arthritis: mechanisms involved in arthrotropism and sustained therapeutic efficacy. *Arthritis Res. Ther.* **2010**, *12* (5), R170.